PNAS
www.pnas.org

Supplementary Information for

Functional Stability of Water Wire-Carbonyl Interactions in an Ion Channel

Joana Paulino, Myunggi Yi, Ivan Hung, Zhehong Gan, Xiaoling Wang, Eduard Y. Chekmenev, Huan-Xiang Zhou, Timothy A. Cross

Corresponding Author: Timothy A. Cross
Email: cross@magnet.fsu.edu

This PDF file includes:

www.pnas.org/cgi/doi/10.1073/pnas.2001083117

Supplementary Information Text

The structure of gramicidin A (gA) is a symmetric dimer (Fig. S1). The formyl blocked amino-termini at the bilayer center and the ethanolamine blocked carboxy-termini at the bilayer surface results in both monomers being in identical environments leading to identical gA structures for the two monomers (1). While only a couple of the gA backbone sites have been characterized at 1.5 GHz (2), the all atom high resolution structure of the gA dimer was characterized with spectral restraints from ^{15}N, ^{13}C and ^{2}H labeled sites (3). Using oriented sample solid-state NMR and orientation dependent anisotropic chemical shifts, quadrupolar and dipolar interactions from throughout the peptide led to a high resolution structure and a complete cross-validation and R factor calculation for the structure (4). The rms deviation for the motionally averaged structure was 0.11Å among the backbone atoms (4). Below (Fig. S2) is the dataset of anisotropic ^{15}N chemical shifts that are very sensitive to structural perturbations and yet show no evidence of asymmetry from the specific site labeled samples of gA in liquid crystalline lipid bilayers (5). Unlike an α-helix, but like a β-strand structure the gA peptide planes alternate between two orientations, one in which the N→H vector is oriented toward the N-terminus (the L-residues) and the other in which this vector is oriented toward the C-terminus (Glycine and the D-residues). The ^{2}H quadrupolar couplings for the indole sidechains and the other aliphatic side chains were recorded characterizing high resolution structures (Fig. S3, 6,3). The complete structure with all sidechains characterized was submitted to the PDB (1MAG) as the first PDB submission based on solid state NMR spectroscopy.

Note that the ^{15}N chemical shifts for Figures S2 and S3 and Table S1 are different from those in this manuscript because of a 26.8 ppm difference in the present generally accepted chemical shift reference.

^{17}O Lineshape fitting, Shift Calculations and ^{15}N resonances calculation

The fitting of the ^{17}O spectra (Fig. S5 and S6) and the calculation of ^{17}O shifts (Fig. 3) were done by numeric simulation using MatLab. The fitting algorithm took into consideration data acquisition parameters, such as field, dwell time and the line broadening applied during processing. The fittings used and required inputs for the CSA, quadrupolar coupling, asymmetry value, tensor orientation, angle between the C=O bond and the magnetic field and two mosaic spread components simulated as Gaussian distributions. The script took the input of librationally averaged CSA values and calculated an axially symmetric spectrum. The conversion of the DFT parameters to ^{17}O shifts used inputs for the CSA, quadrupolar coupling, asymmetry value and tensor orientations generated by the GIAO method. The angle between the C=O bond and the magnetic field was derived from the 1MAG structure.

For Fig. S6 the ^{15}N data back calculation was based on a hypothesis that the second peak in the ^{17}O spectra for G2 and L10 might be due to changes in the C=O bond orientation with respect to the magnetic field. We used the lineshape fitting calculation described above, but instead of fixing the structural parameters we fixed the CSA for the higher ppm peak and varied the C=O angles for the upfield shifted peaks of G2 and L10. These were determined to be 32° and 21.5°, which resulted in peptide plane tilt angles of 21° and 10°, respectively. The resonances for these predicted A3 and W11 ^{15}N sites were calculated in MatLab using a previously described method (7).

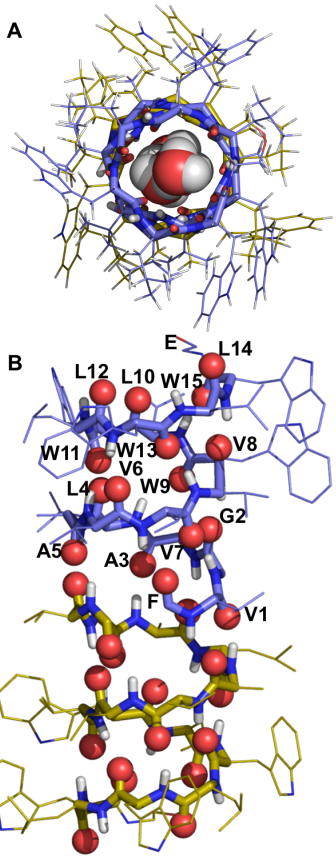

Fig. S1. The N-terminus to N-terminus dimeric gramicidin A channel structure (PDB:1MAG) (1, 3). (A) End view showing the β-strand backbone (sticks) lining the aqueous pore and sidechains (lines) that interact with the fatty acyl chains of the lipids. The amino acid sequence is blocked at either end with a formyl (F) and an ethanolamine (E) group and has alternating D and L amino acids starting with a formylated L-valine residue (fVGALAVVVWLWLWLWe). (B) Side view, highlighting the N-terminus to N-terminus stacking of the two antiparallel monomers, one color-coded with blue carbons and the lower one with gold carbons. The carbonyl oxygens lining the 4 Å diameter pore facilitating cation transport are highlighted as red spheres.

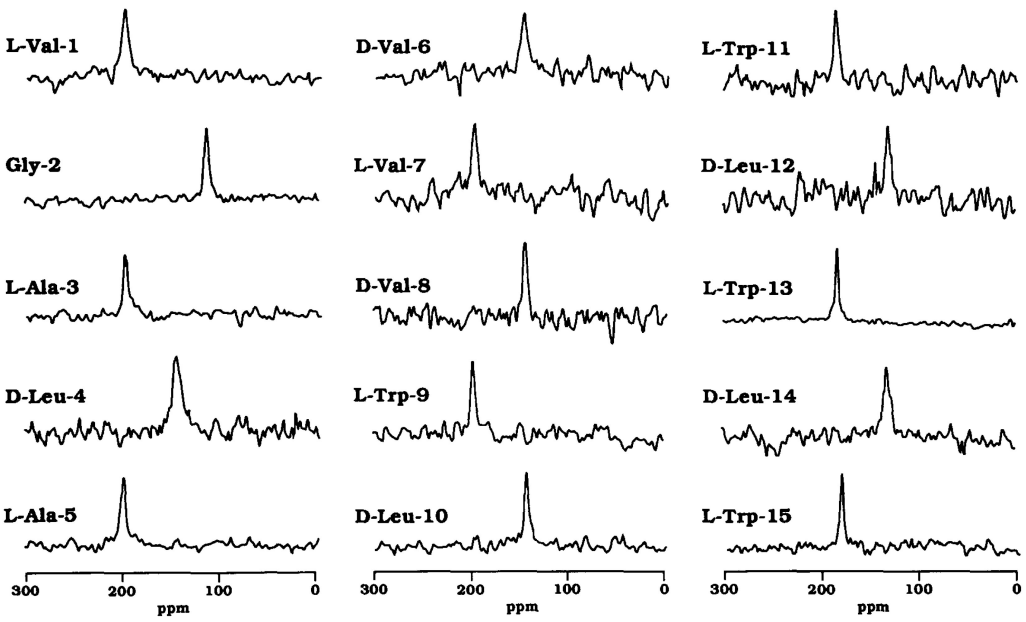

Fig. S2. Anisotropic ^{15}N chemical shift spectra of uniformly oriented gA in liquid crystalline lipid bilayers. The bilayer normal was aligned parallel to the magnetic field axis. Reproduced with permission from (5).

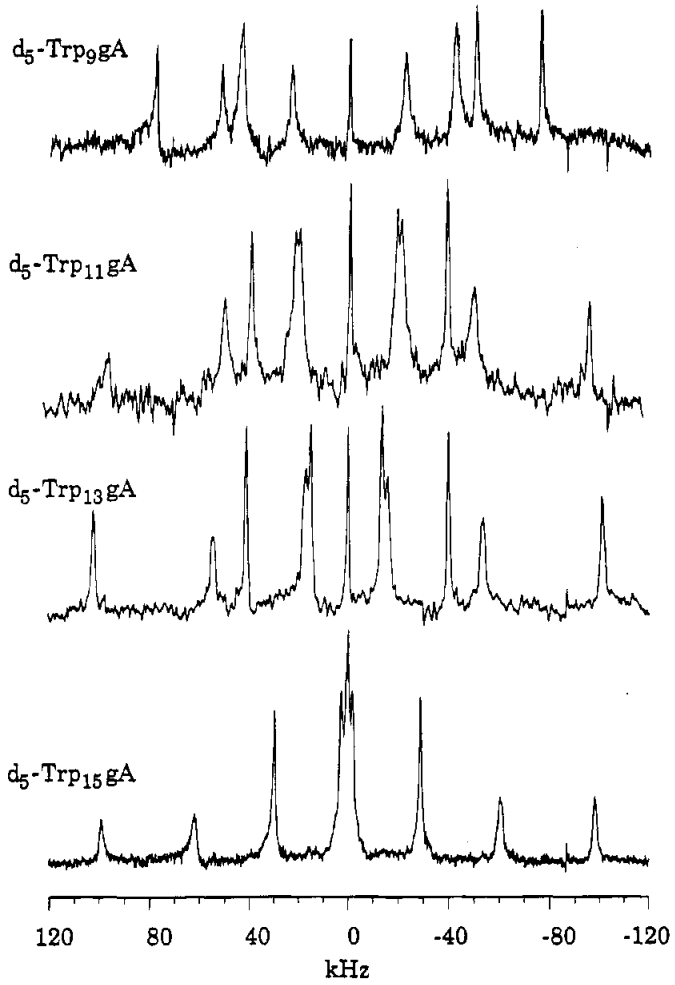

Fig. S3. ^{2}H NMR spectra of W-*d*5 labeled gramicidin A in uniformly aligned bilayers at room temperature. For W11, W13, W15, five quadrupolar splittings can be identified. For W9, only four splittings can be absolutely identified, although the splitting at 85 kHz appears to represent two resonances. These sharp resonances yield very high resolution orientational restraints and document the small mosaic spread (±0.3°) for the orientation of the channel with respect to the magnetic field. Reproduced with permission from (6).

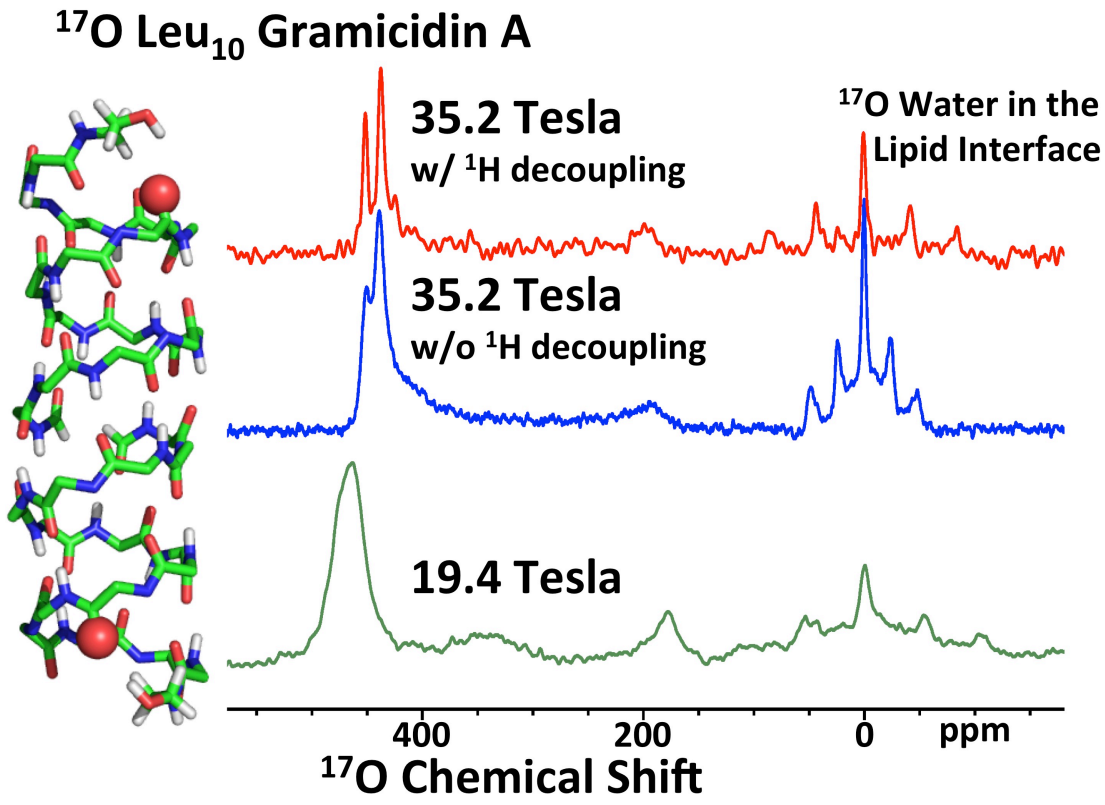

Fig. S4. A comparison of resolution enhancement achieved by going to 35.2 T versus prior spectra obtain at 19.6 T (830 MHz for ^{1}H) in the absence of decoupling. The ^{17}O anisotropy can be observed to range from 460 ppm to 170 ppm at 19.6 T and from 450 ppm to 180 ppm at 35.2 ppm depending on which resonance is considered. The addition of 30 kHz decoupling on the proton channel at 35.2 T clearly unveils the presence of two peaks. It is clear from these spectra that the alignment is not perfect – there is some powder pattern intensity from sample that is not between the glass slides used for alignment or from alignment defect structures in the sample. In addition, it is also clear that there is some mosaic spread of alignment, meaning that the sample is not perfectly aligned but has a small dispersion of orientations with respect to the magnetic field. This influences the simulation of the resonances for quantitating the fraction of sample in each of the resonances. It should also be noted that a natural abundance water resonance is observed as well.

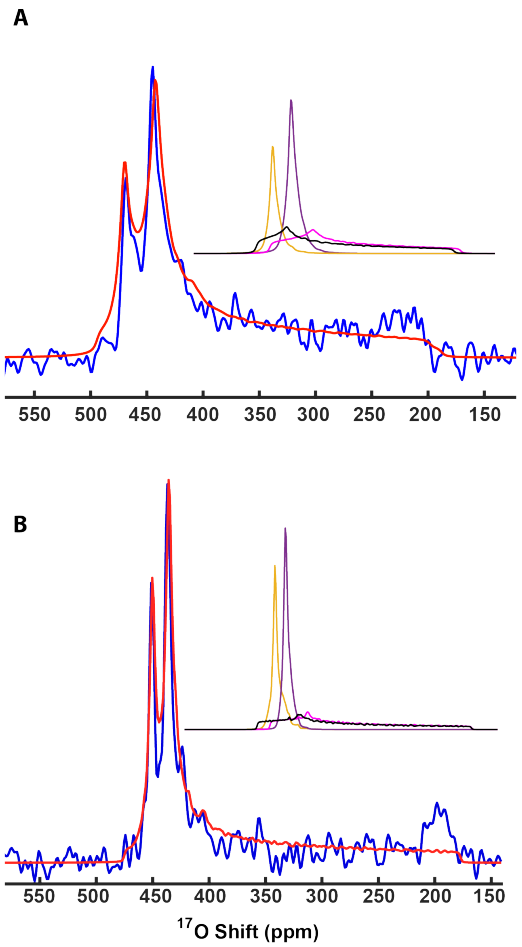

Fig. S5. Lineshape analysis of ^{17}O spectra of gramicidin A labeled at one of two sites: (A) G_2 and (B) L_{10}. In A and B both peaks corresponding to the aligned portion of the samples were fitted using a C=O bond orientation with respect to the magnetic field of 80° as in the PDB structure, 1MAG. Fitting parameters for A (exponential decay of 1 kHz used for data processing also included for fitting): experimental peak at 468 ppm (calculated 468.1 ppm) fitted with motional averaged CSA [210, 440, 485] (ppm), quadrupolar coupling (QC) 7.0 MHz, asymmetry 0.05, tensor orientation [75°, 41°, -80°], mosaic spread for sharp component 1.5° with 6% of an underlying broad component at 10°. Experimental peak at 444 ppm (calculated 441.7 ppm) with motional averaged CSA [200, 400, 465] (ppm), QC 7.0 MHz, asymmetry 0.05, tensor orientation [75°, 41°, -80°], mosaic spread for sharp component 2° with 10% of an underlying broad component at 10°. 25% of the spectral intensity could be fitted to a sum of powder patterns of each component. Fitting parameters for B (exponential decay of 200 Hz used for data processing also included on the fitting): peak at 451 ppm (calculated 450.3 ppm) with motional averaged CSA [190, 400, 470] (ppm), QC 7.3 MHz, asymmetry 0.1, tensor orientation [-81°, 40°, 73°], mosaic spread for sharp component 2° with 8% of an underlying broad component at 10°. Peak at 437 ppm (calculated 435.9 ppm) with motional averaged CSA [190, 390, 452] (ppm), QC 7.3 MHz, asymmetry 0.1, tensor orientation [-81°, 40°, 73°], mosaic spread for sharp component 2° with 15% of an underlying broad component at 8°. 8.5% of the spectral intensity could be fitted to a sum of powder patterns of each component. Inset for A and B: the decomposition of each respective spectral simulation; in purple and yellow the aligned components for the site hydrogen bonded to water and non-hydrogen bonded to water, respectively. In magenta and black the powder patterns for the purple and yellow spectra, respectively.

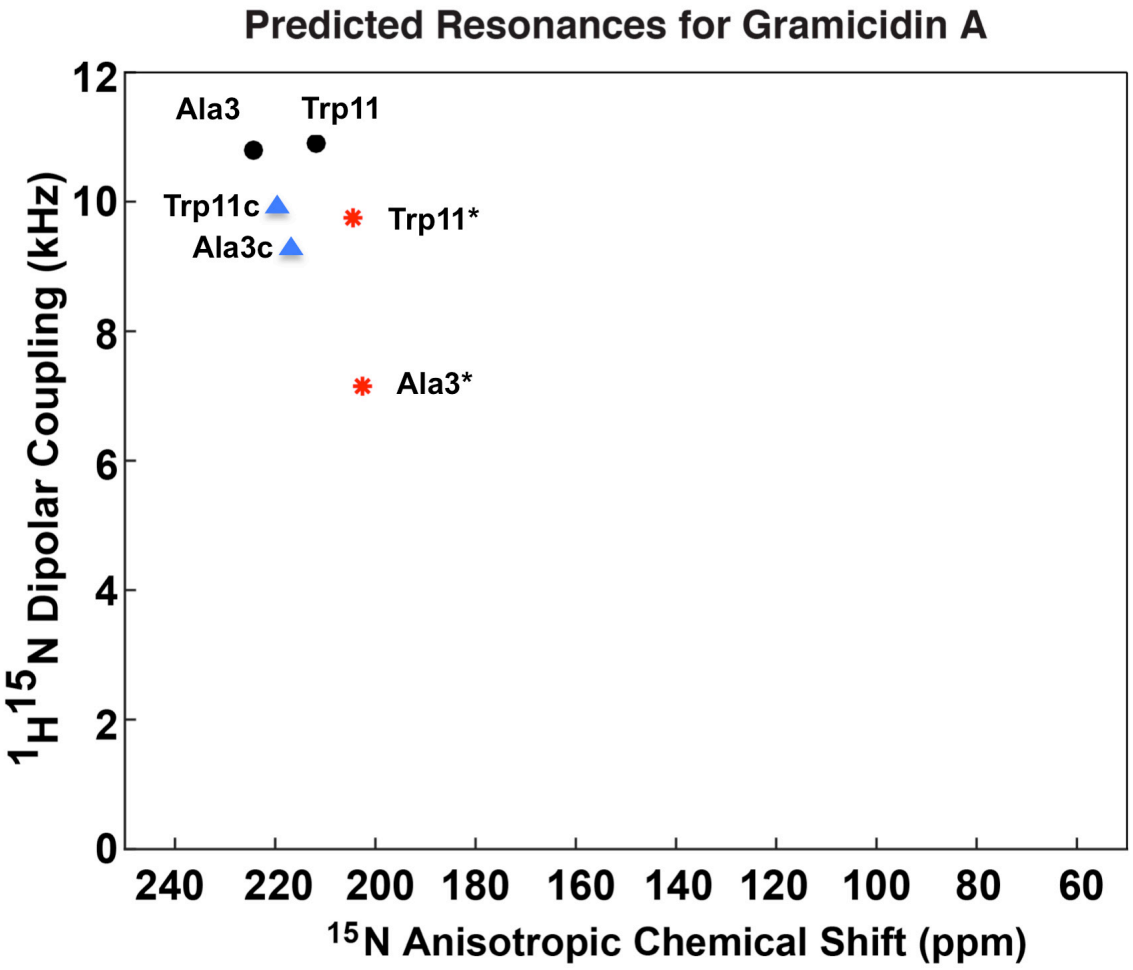

Fig. S6. Comparison of anisotropic ^{15}N chemical shifts and ^{15}N-^{1}H dipolar coupling for the two peptide planes that include the carbonyls from G_2 and L_{10}, calculated in three ways. The black circles are the predictions from the original gA structure (PDB: 1MAG), which, as expected, is in excellent agreement with the original data (A_3 at 224 ± 1 ppm and 10.9 ± 1 kHz) and with the data acquired at 35 T (222 ± 1 ppm and 10.7 ± 0.3 kHz). The blue triangles represent the predictions from the intertwined double helical structure of gA (PDB: 2XDC). Such a structure has not been observed in membrane environment. Red stars are the predicted resonances for the A_3 and W_{11} NH sites considering that the (upfield) shifts in the ^{17}O spectra are due to changes in the peptide plane orientation. The tilts in the peptide planes required to achieve such shifts in the ^{17}O spectra were 21.6˚ for the G_2/A_3 plane and 10˚ for the L_{10}/W_{11} plane. This demonstrates that the changes in the ^{17}O data cannot be due to different conformations of the peptide planes for the observed sites, since the predicted chemical shift and dipolar couplings fall outside of the experimental ^{15}N error bars, even for the W_{11} data, which has larger error bars (±1 kHz) because the data was recorded at much lower field.

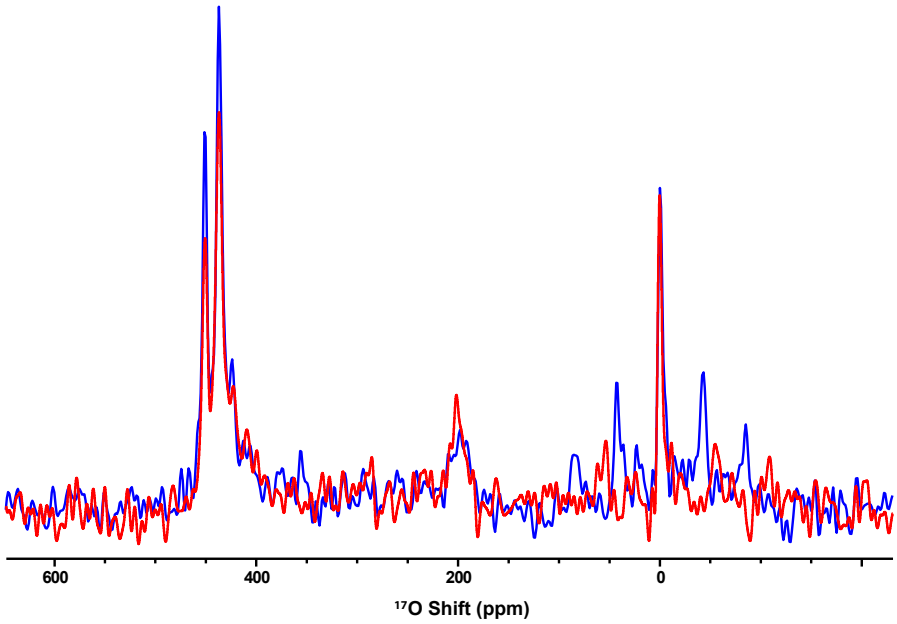

Fig. S7. Comparison of ^{17}O labeled L_{10} gA OS ssNMR spectra obtained at 35.2 T and 30°C (blue) as in Fig. 3, Fig. S4 and Fig. S5 and at 52°C (red). This shows that there is no change in resonance frequencies for these two carbonyl oxygens or in the ^{17}O anisotropy for these carbonyls as indicated by the resonance feature near 200 ppm. Clearly, the flip rate of the water wire orientation in this sample at 52°C is not fast on the timescale of the separation of the two resonances near 450 ppm.

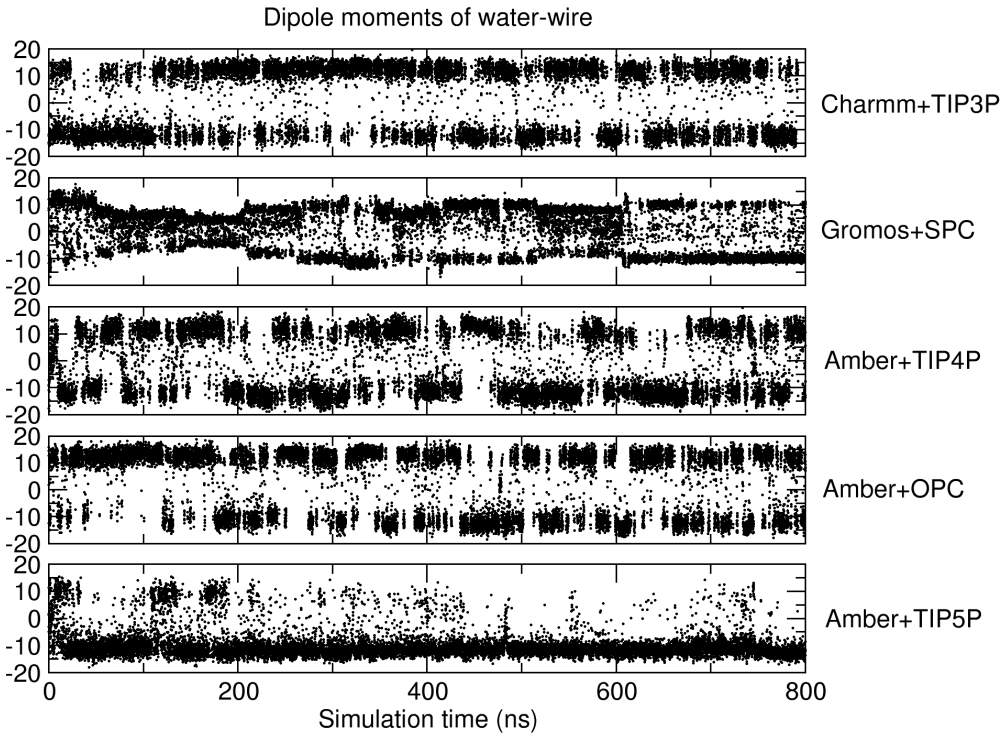

Fig. S8. Electrical dipole moments of the water-wire in the pore, projected along the channel axis, calculated along the simulation time. The labels of the y-axis indicate the dipole moments in Debye unit. Five classical MD simulations were performed with various force fields and water models. Fast flipping of dipole orientation indicates the limitation of the current fixed charge water models to describe the water wire confined in the pore.

Table S1. Orientational constraints from solid-state NMR observations of uniformly aligned samples. Error bars are ±1 ppm for ^{15}N chemical shift data, ±1 kHz for the ^{15}N-^{1}H dipolar interactions, and ±0.03 kHz for the ^{15}N-^{13}C dipolar interactions. For the indole side chains ^{2}H quadrupolar couplings were used (± 1kHz): for W9, $\delta 1$= 46, $\zeta 2$ = 85, $\eta 2$ = -102, $\zeta 3$= 155, and $\varepsilon 3$ = 87; for W11. $\delta 1$ = 77, $\zeta 2$ = 39, $\eta 2$ = -99, $\zeta 3$ = 192, and $\varepsilon 3$ = 43; for W13, $\delta 1$= 108, $\zeta 2$ = 28, $\eta 2$ = -81, $\zeta 3$ = 201, and $\varepsilon 3$ =32; and for W15, $\delta 1$ =123, $\zeta 2$ = 1, $\eta 2$ = -59, $\zeta 3$=198, and $\varepsilon 3$=4. Reproduced with permission from (1).

Site	^{15}N chemical shift (ppm)	Dipolar interaction	
		^{15}N-^{1}H (kHz)	^{15}N-^{13}C (kHz)
Val[1]	198	19.7	0.463
Gly[2]	113	17.6	0.910
Ala[3]	198	21.8	0.670
D-Leu[4]	145	17.2	0.820
Ala[5]	198	20.7	0.572
D-Val[6]	145	18.2	0.626
Val[7]	196	22.0	0.519
D-Val[8]	145	17.8	0.702
Trp[9]	198	20.7	0.487
	145*	13.2*	
D-Leu[10]	144	13.5	†
Trp[11]	185	20.9	0.365
	144*	11.1*	
D-Leu[12]	132	16.2	0.779
Trp[13]	182	20.9	0.454
	144*	10.1*	
D-Leu[14]	131	14.3	0.657
Trp[15]	181	20.9	0.507
	139*	7.7*	

*These results are for the $^{15}N\epsilon_1$ site of the side chain. †Relaxation parameters for this site have compromised our ability to obtain the dipolar coupling.

References

1. R.R. Ketchem, W. Hu, & T.A. Cross, High Resolution Conformation of Gramicidin A in a Lipid Bilayer by Solid-State NMR. *Science* **261**, 1457-1460 (1993).
2. Z. Gan, I. Hung, X. Wang, J. Paulino, G. Wu*, et al.*, NMR spectroscopy up to 35.2T using a series-connected hybrid magnet. *Journal of Magnetic Resonance* **284**, 125-136 (2017).
3. R.R. Ketchem, B. Roux, & T.A. Cross, High-resolution polypeptide structure in a lamellar phase lipid environment from solid state NMR derived orientational constraints. *Structure* **5**, 1655-1669 (1997).
4. S. Kim, J.R. Quine, & T.A. Cross, Complete Cross-Validation and R-Factor Calculation of a Solid-State NMR Derived Structure. *J. Am. Chem. Soc.* **123**, 7292-7298 (2001).
5. W. Mai, W. Hu, C. Wang, & T.A. Cross, Orientational constraints as three-dimensional structural constraints from chemical shift anisotropy: The polypeptide backbone of gramicidin A in a lipid bilayer. *Protein Science* **2**, 532-542 (1993).
6. W. Hu, N.D. Lazo, & T.A. Cross, Tryptophan Dynamics and Structural Refinement in a Lipid Bilayer Environment – Solid-State NMR of the Gramicidin Channel. *Biochemistry* **34**, 14138-14146 (1995).
7. Dylan T. Murray, C. Li, F.P. Gao, H. Qin, & Timothy A. Cross, Membrane Protein Structural Validation by Oriented Sample Solid-State NMR: Diacylglycerol Kinase. *Biophys. J.* **106**, 1559-1569 (2014).